INTERNATIONAL JOURNAL OF HYDROGEN ENERGY 40 (2015) 6552–6558

Available online at www.sciencedirect.com

ScienceDirect

journal homepage: www.elsevier.com/locate/he

Ultrathin MoS_2-coated carbon nanospheres as highly efficient electrocatalyts for hydrogen evolution reaction

Wen-Hui Hu [a], Guan-Qun Han [a,b], Yan-Ru Liu [a], Bin Dong [a,b,*], Yong-Ming Chai [a], Yun-Qi Liu [a], Chen-Guang Liu [a,*]

[a] State Key Laboratory of Heavy Oil Processing, China University of Petroleum (East China), Qingdao 266580, PR China

[b] College of Science, China University of Petroleum (East China), Qingdao 266580, PR China

ARTICLE INFO

Article history:
Received 4 December 2014
Received in revised form
18 March 2015
Accepted 27 March 2015
Available online 15 April 2015

Keywords:
MoS_2
Electrocatalyst
Hydrogen evolution reaction
Carbon nanospheres

ABSTRACT

The ultrathin MoS_2-coated carbon nanospheres have been prepared by a facile solvothermal method using acid-treated carbon nanospheres (ATCNS) as support. TEM images show that ATCNS are homogeneously coated by MoS_2 layers. The thickness of MoS_2 coating on ATCNS is about 5 nm. XRD data confirm that the few stacking layers and low crystalline of MoS_2 nanosheets on ATCNS, which could provide more active sites for hydrogen evolution reaction (HER). The electrocatalytic activity and stability of MoS_2/ATCNS for HER have been investigated. The results show that MoS_2/ATCNS has better electrocatalytic activity for HER than pure MoS_2. It can be speculated that ATCNS play crucial role in increasing conductivity and electrocatalytic activity for HER of MoS_2/ATCNS. The nanostructure of ultrathin MoS_2 coating on ATCNS is a promising electrocatalyts for HER.

Copyright © 2015, Hydrogen Energy Publications, LLC. Published by Elsevier Ltd. All rights reserved.

Introduction

Hydrogen has been pursued to be one of the most promising energy carriers for the effective conversion and utilization of the sustainable resources such as solar energy, wind energy and waterpower [1–3]. Recently, water splitting using electrochemistry [4–7] or photoelectrochemistry cells [8–12] has been widely investigated as valid ways for hydrogen evolution reaction (HER). The most efficient electrocatalysts for water splitting are noble metals, such as Pt. The obvious disadvantage of noble metals is the high price and limited reserves which are big barriers for widely industrial utilization [13]. Therefore, the exploration of high efficient HER electrocatalysts from earth-abundant elements has become a global hot research. In fact, various noble-metal-free catalysts including transition metal sulfides [14,15], oxides [16], and compounds [17,18] have been widely developed to partially substitute the role of Pt in water splitting. Some substitutes with rich earth-abundance have demonstrated high activity close to that of Pt, but there are still some challenges to improve their catalytic

* *Corresponding authors*. State Key Laboratory of Heavy Oil Processing, China University of Petroleum (East China), Qingdao 266580, PR China. Tel.: +86 532 86981376; fax: +86 532 86981787.
E-mail addresses: dongbin@upc.edu.cn (B. Dong), cgliu.upc.edu.cn@gmail.com (C.-G. Liu).
http://dx.doi.org/10.1016/j.ijhydene.2015.03.150
0360-3199/Copyright © 2015, Hydrogen Energy Publications, LLC. Published by Elsevier Ltd. All rights reserved.

efficiency and stability to meet the practical requirements of industrial application [19].

Among these candidates, molybdenum disulfide (MoS_2) nanomaterials have showed good electrocatalytic activity for HER, which has been confirmed by the computational and experimental results [20,21]. The active sites of MoS_2 are mainly the rims and edges of MoS_2 nanosheets rather than the basal planes [22], and it is proportional to the electrocatalytic activity for HER. However, as a typical two-dimensional (2D) transition-metal sulfide, MoS_2 has analogous layered structure of graphene, which are vulnerable to result in severe stacking and aggregation owing to the high surface energy and interlayer van der Waals attraction [23]. The obvious stacking and aggregation phenomena will decrease the number of the active sites for HER. Another disadvantage of MoS_2 is the poor conductivity because of the semi-conductive nature, in which the electrons prefer to transfer along the lamella structure of MoS_2 nanosheets. Therefore, designing suitable nanostructures of MoS_2 with the more exposed active sites, as well as improving of the conductivity of MoS_2 by using ideal supports, is the key to improve the properties of MoS_2-based electrocatalysts for HER effectively.

Owing to the excellent conductivity and stability, carbon nanomaterials as support for MoS_2-based electrocatalysts have been widely studied including graphene [24,25], reduced graphene oxide [26,27], carbon nanotubes [28], carbon nanospheres (CNS) [29]. These researches have confirmed that carbon nanomaterials could improve the exposed active sites and conductivity of MoS_2. However, there remain some problems such as cost barrier, complicated procedures, aggregation growth of MoS_2 etc. In this work, a facile solvothermal method using situ hydrolysis of ammonium thiomolybdate ($(NH_4)_2MoS_4$) in N, N-dimethylformamide (DMF) has been developed to prepare ultrathin MoS_2-coated acid-treated carbon nanospheres (MoS_2/ATCNS) with highly homogenous dispersion and low crystalline structure. The results show that as-prepared ultrathin MoS_2/ATCNS nanostructures have the enhanced electrocatalytic activity and stability for HER. The effect of ATCNS and situ hydrolysis of $(NH_4)_2MoS_4$ on the morphology and structure of MoS_2/ATCNS have been discussed.

Experimental

Synthesis of catalysts

Firstly, 80 mg of the acid-treated carbon nanospheres and 80 mg $(NH_4)_2MoS_4$ were dissolved in the solution of 64 mL DMF and 16 mL deionized water under stirring for 1 h and sonication for 1 h. Then the mixture and 0.80 mL hydrazine was transferred into a Teflon stainless steel autoclave. The solvothermal reaction was carried out at the temperature of 200 °C for 12 h. The as-prepared MoS_2/ATCNS were collected by centrifugation and subsequently washed with deionized water and absolute ethanol three times. The products were obtained and dried at 60 °C for 24 h in a vacuum oven. For comparison, the pure MoS_2 and MoS_2/original carbon nanospheres (MoS_2/OCNS) samples have also been synthesized under identical conditions.

Catalysts characterization

Crystallographic structure of all as-prepared samples was investigated with X-ray powder diffraction (XRD, X'Pert PRO MPD, Cu KR) at a scanning rate of 1 °C min^{-1}. XRD data were collected in the 2θ ranges from 5 to 80°. The morphology of the samples was examined with field-emission scanning electron microscopy (SEM, Hitachi, S-4800). Transmission electron microscopy (TEM) images were collected on HRTEM, JEM-2100UHR with an accelerating voltage of 200 kV. The samples were prepared by dropping the ethanol solution of samples on the Cu grids and were observed at 100 kV.

Electrocatalytic measurements for HER

The glassy carbon electrode (GCE) as work electrode with the diameter of 4.0 mm (Gamry Reference 600 Instruments, USA) was polished with alumina slurry and cleaned with ethanol and DI water. A conventional three-electrode system was used with Ag/AgCl as the reference electrode and Pt foil as counter electrode. The potential values are corrected to the reverse hydrogen electrode (RHE) according the equation E (RHE) = E (Ag/AgCl) + 0.22 V. Typically, 4 mg of sample and 20 μL Nafion solution (5 wt%) were dispersed in 1 mL water−ethanol solution with volume ratio of 1:1 by sonicating for 1 h to form a homogeneous ink. Then 10 μL of the dispersion was loaded onto a glassy carbon electrode. The cathodic current density was calculated by the geometric area of GCE which is 0.1256 cm^2. Prior to each electrochemical measurement, the electrolyte solution was purified with N_2 for 30 min to remove the dissolved oxygen, and stable polarization curves were recorded after 10 cycles.

Results and discussion

Fig. 1 shows FT-IR spectra of the original and acid-treated carbon nanospheres. Fig.1a shows that there are only a few oxygen-containing functional groups on the surface of OCNS. In Fig.1b, the peak of 3400 cm^{-1} belongs to hydroxy group. The peaks of 1718, 1583 and 1397 cm^{-1} correspond to carboxyl group on the surface of ATCNS. The large amount of oxygen-containing functional groups on the surface of ATCNS may be very useful for the homogeneous interaction and decreasing stacking layers of MoS_2/ATCNS [24].

Fig. 2 shows SEM images of carbon nanospheres after acid-treatment. The homogeneous morphology and uniform size of ATCNS have also been confirmed. The pure ATCNS with the diameter of about 40 nm has good dispersion, which are very suitable for fabricating MoS_2/ATCNS. SEM images of the original carbon nanospheres (in Fig. S1) reveal that there is no obvious difference in morphology compared with ATCNS, which implies that the acid-treatment does not change the morphology and dispersion of the carbon nanospheres.

Fig. 3 shows the TEM images of ATCNS and MoS_2/ATCNS. Fig. 3a and b shows that the pure ATCNS are highly uniform and well dispersed with the diameter of about 40 nm, which is consistent with the results observed in Fig. 2. Fig. 3c and d shows that MoS_2/ATCNS have uniformly spherical morphology. Fig. 3c indicates that ATCNS is uniformly coated

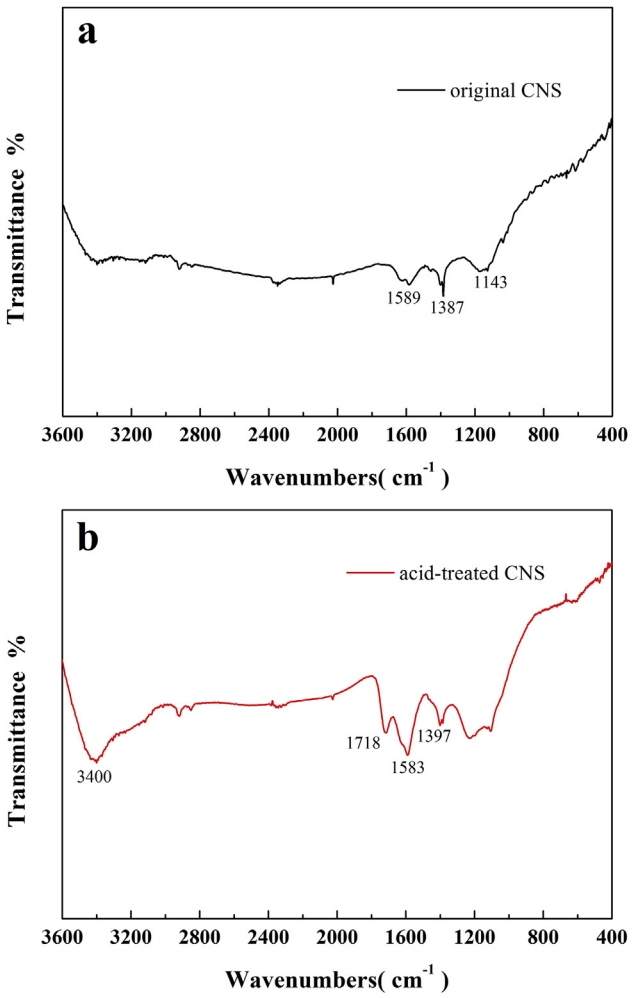

Fig. 1 – FT-IR spectra of the carbon nanospheres. (a) original carbon nanospheres, (b) acid-treated carbon nanospheres.

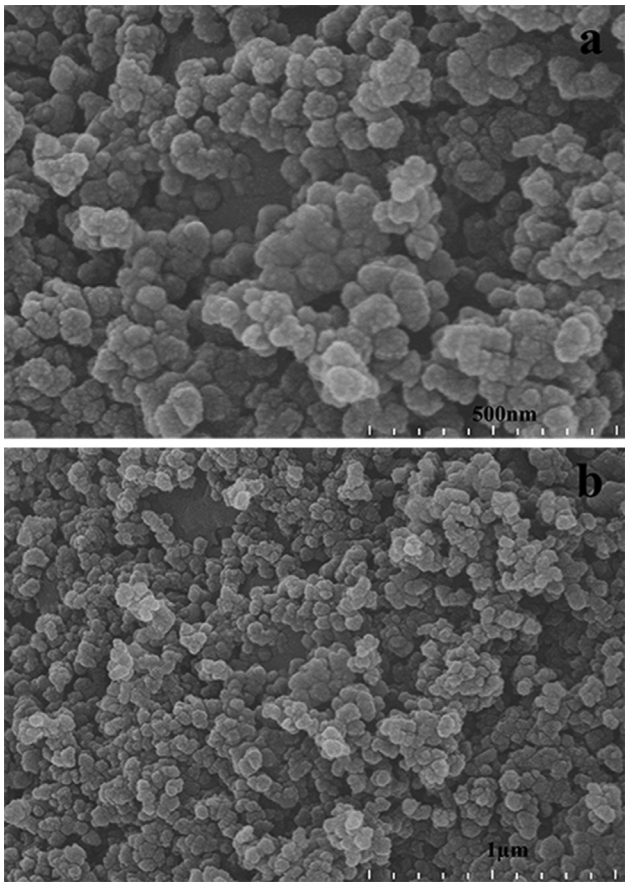

Fig. 2 – SEM images of carbon nanospheres after acid-treatment.

with MoS_2 nanosheets. And the diameter of MoS_2/ATCNS increases to about 50 nm. So the thickness of MoS_2 coating was estimated to be about 5 nm according to the 40 nm diameter of ATCNS, which implies that the staking of MoS_2 on ATCNS has not been severe. Under higher magnification, Fig. 3d shows the ultrathin MoS_2 coating on ATCNS is homogeneous and tight coupling on ATCNS. The aggregation structures of MoS_2 are not observed, which confirms the homogeneous conjunction and few stacking layers of MoS_2. Fig. 3e confirms the thickness and close interaction of ultrathin MoS_2 coating on ATCNS. As shown in Fig. 3f, the ultrathin MoS_2 coating on ATCNS are composed of a few stacking layers (5–8 layers) with the increasing 002 interlayer distance of 0.745 nm, which means low crystalline and weak growth along 002 plane. The homogeneous interaction and decreasing stacking layers of MoS_2/ATCNS may be attributed to the large amount of hydroxy and carboxyl group on the surface of ATCNS. In addition, the situ hydrolysis of $(NH_4)_2MoS_4$ can release H_2S as the sulfur source for the fewer stacking and controllable growth of MoS_2 nanosheets [30,31]. Meanwhile, the effect of DMF and water as solvent on the morphology of MoS_2/ATCNS can be helpful for the good dispersion and controllable growth of MoS_2 nanosheets [28]. For comparison, the as-prepared pure MoS_2 under identical conditions has severe aggregation and many stacking layers (in Fig. S2), which indicating the less active sites and weak activity for HER. From SEM images of MoS_2/ATCNS (in Fig. S3), the obvious aggregation of MoS_2 can't be observed. The stacking layers of MoS_2 are very small, which imply that MoS_2 have better dispersion on ATCNS. Ultrathin layers of MoS_2 with more catalytic active sites have a very good coating on the surface of ATCNS. Therefore, it is meaningful to use ATCNS as support for improving the good dispersion and the increasing the numbers of catalytic active sites of MoS_2.

Fig. 4 shows XRD patterns of pure ATCNS, pure MoS_2 and MoS_2/ATCNS, respectively. The peaks at 25.4°and 43.5°are indexed to (002) and (100) planes of ATCNS in MoS_2/ATCNS, respectively. The peaks at 31.8°and 56.7°are indexed to (100) and (110) planes of MoS_2 in MoS_2/ATCNS, respectively (JCPDS card no.37-1492). No other peaks from impurities have been detected, indicating the high purity of MoS_2/ATCNS. In comparison to the pure MoS_2, the (002) peak of 14.5°of MoS_2 in MoS_2/ATCNS is almost missing, which means the lower crystalline and fewer stacking of MoS_2 nanosheets. In addition, the weak peak of 9.2°for MoS_2/ATCNS means that ATCNS may insert into the MoS_2 layers and expand the interlayer distance of MoS_2 [32], which can be confirmed by Fig. 3f. The less stacking layers and weaker intensity of 002 could provide more rims and edges of MoS_2 as active sites for HER [33].

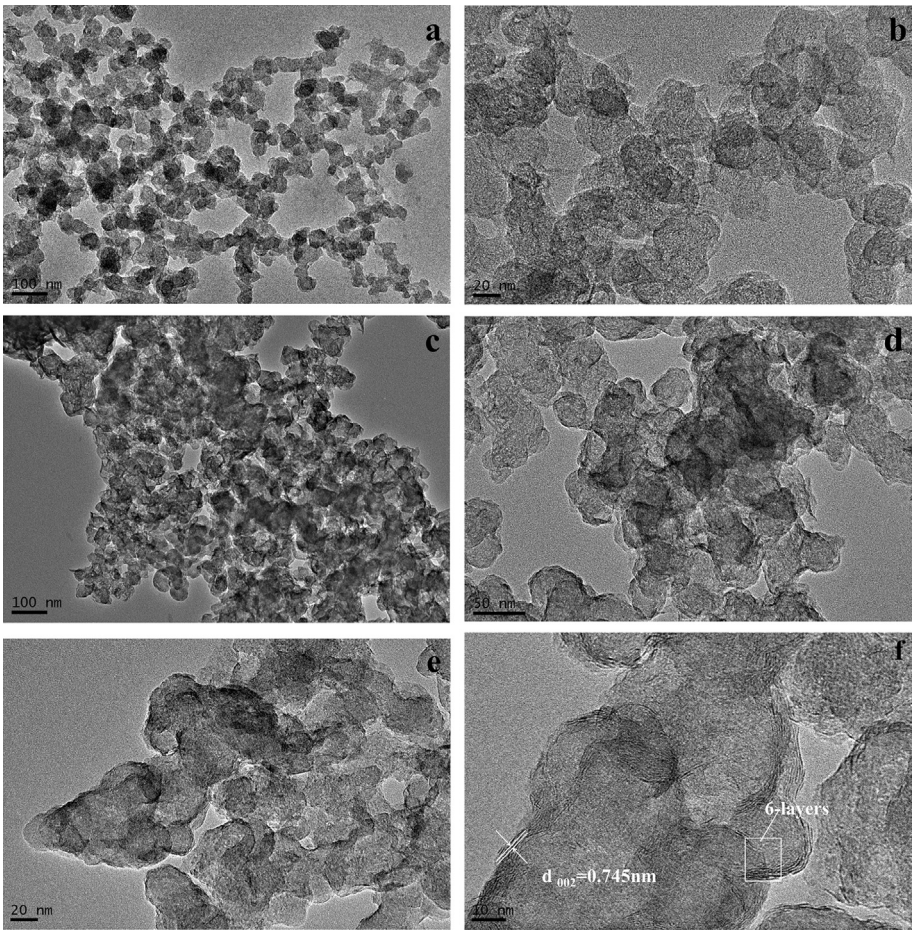

Fig. 3 – (a), (b) TEM images of acid-treated carbon nanospheres. (c), (d), (e) and (f) TEM images of MoS_2/ATCNS.

To demonstrate the electrocatalytic properties of MoS_2/ATCNS for HER, the linear sweep voltammograms (LSV) and tafel plots of the different samples were performed in 0.5 M H_2SO_4 solution (as shown in Fig. 5A). Fig. 5A shows the polarization curves for the different samples including bare glass carbon electrode (GCE), pure MoS_2, MoS_2/ATCNS, MoS_2/OCNS and physical mixture of MoS_2 and ATCNS (MoS_2-ATCNS). It can be observed that MoS_2/ATCNS exhibits good electrocatalytic activity for HER with onset potential of −0.14 V (vs. RHE) and high current densities of ~10 and ~50 mA cm^{-2} at overpotentials of 200 and 240 mV. This onset potential of MoS_2/ATCNS is smaller than that of pure MoS_2, MoS_2/OCNS and MoS_2-ATCNS, which suggests the better electrocatalytic activity for HER. The observed cathodic current densities for pure MoS_2, MoS_2/OCNS MoS_2-ATCNS were much lower. Because the cathodic current density is proportional to the quantity of evolved hydrogen [34], the larger current density of MoS_2/ATCNS indicates the better HER electrocatalytic behaviour, which may be attributed to the improved conductivity, the homogeneous interaction and ultrathin MoS_2 coating on the surface of ATCNS.

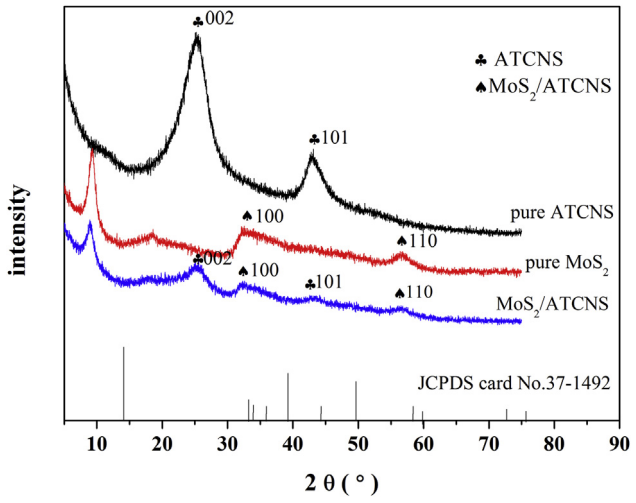

Fig. 4 – XRD patterns of different samples: pure ATCNS, pure MoS_2 and MoS_2/ATCNS.

The ideal electrocatalysts should have low Tafel slopes and high cathodic current densities. Pt has a high current density in the order of 10^{-3} A cm^{-2} and a Tafel slope of 30 mV dec^{-1} for HER [5]. Fig. 5B shows Tafel slopes of 53, 54 and 55 mV dec^{-1} for MoS_2/ATCNS, MoS_2-ATCNS and MoS_2/OCNS, respectively. MoS_2/ATCNS display the best electrocatalytic activity with the smallest slope value of 53 mV dec^{-1}, which is similar to the previous report [35]. For HER mechanism, the first step is a fast discharge reaction (Equation (1)) and the rate determining step is the electrochemical desorption of H_{ads} and H_3O^+ to form

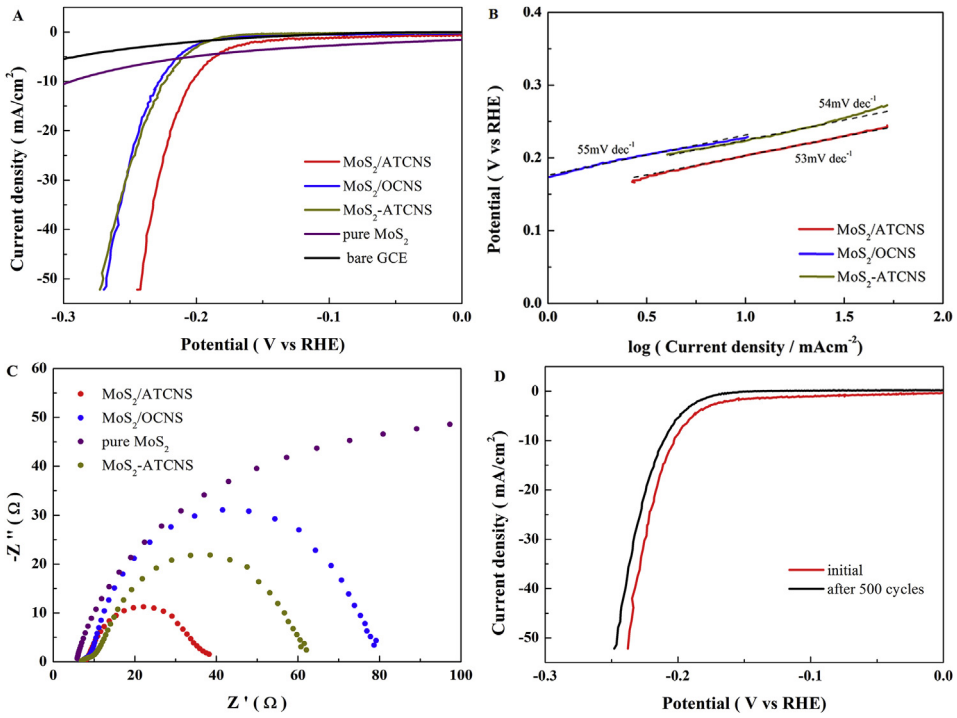

Fig. 5 – (A) Linear sweep voltammogram curves in 0.5 M H_2SO_4 for different electrocatalysts. The scan rate is 20 mV s^{-1} and the scan region ranges from 0 to −0.3 V vs RHE, (B) Tafel plots of different electrocatalysts, (C) AC impedance spectra for different electrocatalysts at overpotential of 0.2 V from 10^5 to 0.1 Hz with an AC voltage of 5 mV, (D) Stability for the MoS_2/ATCNS composite modified electrode with initial polarization curve (red curve) and after 500 cycles (black curve). (For interpretation of the references to colour in this figure legend, the reader is referred to the web version of this article.)

hydrogen (Equation (2)), which complies with Volmer–Heyrovsky mechanism [36,37].

$$\text{Volmer reaction: } H_3O^+ + e \rightarrow H_{ads} + H_2O \quad (1)$$

$$\text{Heyrovsky reaction: } H_3O^+ + e + H_{ads} \rightarrow H_2 + H_2O \quad (2)$$

The conductivity of different samples can be measured by AC impedance (in Fig. 5C). MoS_2/ATCNS shows much smaller charge-transfer resistance than pure MoS_2, MoS_2/OCNS and MoS_2-ATCNS. The enhancement of conductivity also benefits from the homogeneous conjunction between ATCNS and MoS_2. The smaller resistance means much faster electron transfer and improved efficiency in HER.

The long-term stability of electrocatalysts is an important requirement for industrial application. A long-term potential sweep of MoS_2/ATCNS was performed from −0.3 to 0 V vs. RHE (Fig. 5D). The LSV retained similar current density to the initial one and a slight loss could be observed after 500 cycles, indicating that MoS_2/ATCNS has good stability for HER.

From FR-IT data, ATCNS have more oxygen-containing functional groups, which is very useful for improving the growing of ultrathin MoS_2 on carbon nanospheres (in Fig. 3). The good coating of MoS_2/ATCNS means better conductivity. A few stacking layers of MoS_2/ATCNS would provide more active sites for HER. Therefore, MoS_2/ATCNS sample should have the better HER activity. To obtain further insight into the electrocatalytic activity of MoS_2/ATCNS, exchange current densities of various catalysts have been investigated (Fig. 6). The exchange current densities of various samples were calculated by using extrapolation methods (Table 1). The resulting exchange current densities of MoS_2/ATCNS samples is 2.57 μA cm^{-2}, which is larger than 0.65 μA cm^{-2} of MoS_2/OCNS and 0.68 μA cm^{-2} of MoS_2-ATCNS. The exchange

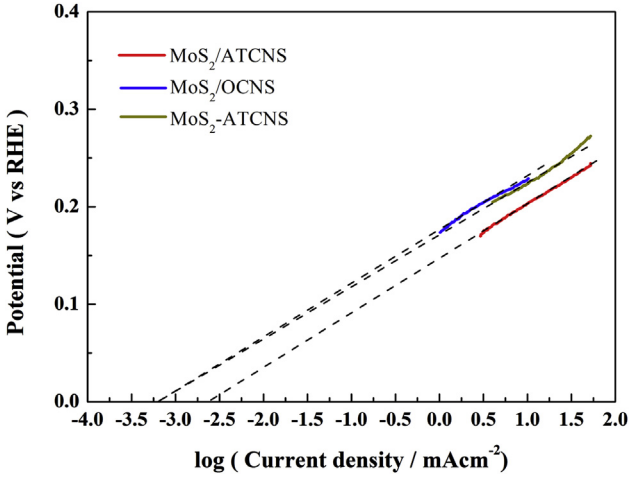

Fig. 6 – Calculated exchange current densities of various samples by using extrapolation methods.

Table 1 – Calculations of the exchange current densities of various samples.

Materials	Log (Current density/ mA cm^{-2}) at $\eta = 0$ V	Exchange current densities j_0 ($\mu A/cm^2$)
MoS_2/ ATCNS	−2.59	2.57
MoS_2/ OCNS	−3.19	0.65
MoS_2- ATCNS	−3.17	0.68

current densities confirmed that MoS_2/ATCNS have the better electrocatalytic behaviour for HER.

Conclusion

In conclusions, ultrathin MoS_2/ATCNS with homogenous dispersion and close interaction has been fabricated by a facile solvothermal method. The TEM showed the thickness of ultrathin MoS_2 coating on ATCNS is about 5 nm. XRD confirmed the few stacking layers and low crystalline of MoS_2 nanosheets, which could provide more active sites for HER. It can be speculated that both ATCNS and situ hydrolysis of $(NH_4)_2MoS_4$ play crucial role in improving conductivity and preparing ultrathin MoS_2 coating of MoS_2/ATCNS. The good conductivity means the fast electron transport between the active site and the electrode. The few stacking layers mean that there are more exposed active sites on the surface of MoS_2/ATCNS. According to the LSV and exchange current densities results, MoS_2/ATCNS have the better electrocatalytic activity for HER. Therefore, the nanostructure of ultrathin MoS_2 coating on ATCNS is a promising choice to prepare highly efficient electrocatalysts for HER.

Acknowledgements

This work is financially supported by the National Natural Science Foundation of China (No.U1162203) and the National Natural Science Foundation of China (No. 21106185).

Appendix A. Supplementary data

Supplementary data related to this article can be found at http://dx.doi.org/10.1016/j.ijhydene.2015.03.150.

REFERENCES

[1] Lewis NS. Toward cost-effective solar energy use. Science 2007;315:798–801.
[2] Armaroli N, Balzani N. The future of energy supply: challenges and opportunities. Angew Chem Int Ed 2007;46:52–66.
[3] Joshi AS, Dincer I, Reddy BV. Exergetic assessment of solar hydrogen production methods. Int J Hydrogen Energy 2010;35:4901–8.
[4] Mitov M, Chorbadzhiyska E, Rashkov R, Hubenova Y. Novel nanostructured electrocatalysts for hydrogen evolution reaction in neutral and weak acidic solutions. Int J Hydrogen Energy 2012;37:16522–6.
[5] Vrubel H, Merki H, Hu XL. Hydrogen evolution catalyzed by MoS_3 and MoS_2 particles. Energy Environ Sci 2012;5:6136–44.
[6] Zhang L, Wu HB, Yan Y, Wang X, Lou XW (David). Hierarchical MoS_2 microboxes constructed by nanosheets with enhanced electrochemical properties for lithium storage and water splitting. Energy Environ Sci 2014;7:3302–6.
[7] Tang CY, Wang DZ, Wu ZZ, Duan BH. Tungsten carbide hollow microspheres as electrocatalyst and platinum support for hydrogen evolution reaction. Int J Hydrogen Energy 2015;40:3229–37.
[8] Grätzel M. Photoelectrochemical cells. Nature 2001;414:338–44.
[9] Tang ML, Grauer DC, Lassalle-Kaiser B, Yachandra VK, Amirav L, Alivisatos AP. Structural and electronic study of an amorphous MoS_3 hydrogen-generation catalyst on a quantum-controlled photosensitizer. Angew Chem Int Ed 2011;50:10203–7.
[10] Maitra U, Gupta U, De M, Datta R, Govindaraj A, Rao CNR. Highly effective visible-light-induced H_2 generation by single-layer 1T-MoS_2 and a nanocomposite of few-layer 2H-MoS_2 with heavily nitrogenated graphene. Angew Chem Int Ed 2013;52:13057–61.
[11] Sharma V, Kumar P, Singh N, Upadhyay S, Satsangi VR, Dass S, et al. Photoelectrochemical water splitting with nanocrystalline $Zn_{1-x}Ru_xO$ thin films. Int J Hydrogen Energy 2012;37:12138–49.
[12] Yan ZP, Wu HT, Han AL, Yu XS, Du PW. Noble metal-free cobalt oxide (CoO_x) nanoparticles loaded on titanium dioxide/cadmium sulfide composite for enhanced photocatalytic hydrogen production from water. Int J Hydrogen Energy 2014;39:13353–60.
[13] Chen WF, Muckerman JT, Fujita E. Recent developments in transition metal carbides and nitrides as hydrogen evolution electrocatalysts. Chem Commun 2013;49:8896–909.
[14] Cheng L, Huang WJ, Gong QF, Liu CH, Liu Z, Li YJ, et al. Ultrathin WS_2 nanoflakes as a high-performance electrocatalyst for the hydrogen evolution reaction. Angew Chem Int Ed 2014;53:7860–3.
[15] Lu ZY, Zhang HC, Zhu W, Yu XY, Kuang Y, Chang Z, et al. In situ fabrication of porous MoS_2 thin-films as high-performance catalysts for electrochemical hydrogen evolution. Chem Commun 2013;49:7516–8.
[16] Phuruangrat A, Hamb DJ, Thongtema S, Lee JS. Electrochemical hydrogen evolution over MoO_3 nanowires produced by microwave-assisted hydrothermal reaction. Electron Commun 2009;11:1740–3.
[17] Zou XX, Huang XX, Goswami A, Silva R, Sathe BR, Mikmekov E, et al. Cobalt-embedded nitrogen-rich carbon nanotubes efficiently catalyze hydrogen evolution reaction at all pH values. Angew Chem Int Ed 2014;53:4372–6.
[18] Yu X, Xu P, Hua T, Han AL, Liu X, Wu H, et al. Multi-walled carbon nanotubes supported porous nickel oxide as noble metal-free electrocatalysts for efficient water oxidation. Int J Hydrogen Energy 2014;39:10467–75.
[19] McKone JR, Marinescu SC, Brunschwig BS, Winkler JR, Gray HB. Earth-abundant hydrogen evolution electrocatalysts. Chem Sci 2014;5:865–78.
[20] Lukowski MA, Daniel AS, Meng F, Forticaux A, Li LS, Jin S. Enhanced hydrogen evolution catalysis from chemically exfoliated metallic MoS_2 nanosheets. J Am Chem Soc 2013;135:10274–7.
[21] Yin ZY, Chen B, Bosman M, Cao XH, Chen JZ, Zheng B, et al. Au nanoparticle-modified MoS_2 nanosheet-based

photoelectrochemical cells for water splitting. Small 2014;10:3537–43.
[22] Norskov JK, Christensen CH. Toward efficient hydrogen production at surfaces. Science 2006;312:1322–3.
[23] Jeffery AA, Nethravathi C, Rajamathi M. Two-dimensional nanosheets and layered hybrids of MoS_2 and WS_2 through exfoliation of ammoniated MS_2 (M = Mo,W). J Phys Chem C 2014;118:1386–96.
[24] Li YG, Wang HL, Xie LM, Liang YY, Hong GS, Dai HJ. MoS_2 nanoparticles grown on graphene: an advanced catalyst for the hydrogen evolution reaction. J Am Chem Soc 2011;133:7296–9.
[25] Liao L, Zhu J, Bian XJ, Zhu L, ScanlonD M, Girault HH, et al. MoS_2 formed on mesoporous graphene as a highly active catalyst for hydrogen evolution. Adv Funct Mater 2013;23:5326–33.
[26] Zheng XL, Xu JB, Yan KY, Wang H, Wang ZL, Yang SH. Space-confined growth of MoS_2 nanosheets within graphite: the layered hybrid of MoS_2 and graphene as an active catalyst for hydrogen evolution reaction. Chem Mater 2014;26:2344–53.
[27] Ma CB, Qi XY, Chen B, Bao SY, Yin ZY, Luo ZM, et al. MoS_2 nanoflower-decorated reduced graphene oxide paper for high-performance hydrogen evolution reaction. Nanoscale 2014;6:5624–9.
[28] Yan Y, Ge XM, Liu ZL, Wang JY, Lee JM, Wang X. Facile synthesis of low crystalline MoS_2 nanosheet-coated CNTs for enhanced hydrogen evolution reaction. Nanoscale 2013;5:7768–71.
[29] Bian XJ, Zhu J, Scanlon MD, Ge PY, Ji C, Girault HH, et al. Nanocomposite of MoS_2 on ordered mesoporous carbon nanospheres: a highly active catalyst for electrochemical hydrogen evolution. Electron Commun 2012;22:128–32.
[30] Chang K, Chen WX. L-cysteine-assisted synthesis of layered MoS_2/graphene composites with excellent electrochemical performances for lithium ion batteries. ACS Nano 2011;5:4720–8.
[31] Zhang L, Lou XW(David). Hierarchical MoS_2 shells supported on carbon spheres for highly reversible lithium storage. Chem Eur J 2014;20:5219–23.
[32] Liu YC, Jiao LF, Wu Q, Du J, Zhao YP, Si YC, et al. Sandwich-structured graphene-like MoS_2/C microspheres for rechargeable Mg batteries. J Mater Chem A 2013;1:5822–6.
[33] Kisielowski C, Ramasse QM, Hansen LP, Brorson M, Carlsson A, Molenbroek AM, et al. Imaging MoS_2 nanocatalysts with single-atom sensitivity. Angew Chem Int Ed 2010;49:2708–10.
[34] Xie JF, Zhang H, Li S, Wang RX, Sun X, Zhou M, et al. Defect-rich MoS_2 ultrathin nanosheets with additional active edge sites for enhanced electrocatalytic hydrogen evolution. Adv Mater 2013;25:5807–13.
[35] Zhao X, Zhu H, Yang XR. Amorphous carbon supported MoS_2 nanosheets as effective catalysts for electrocatalytic hydrogen evolution. Nanoscale 2014;6:10680–5.
[36] Hinnemann B, Moses PG, Nielsen JH, Horch S, Chorkendorff I, Nørskov JK. Biomimetic hydrogen evolution: MoS_2 nanoparticles as catalyst for hydrogen evolution. J Am Chem Soc 2005;127:5308–9.
[37] Morales-Guio CG, Stern LA, Hu XL. Nanostructured hydrotreating catalysts for electrochemical hydrogen evolution. Chem Soc Rev 2014;43:6555–69.